Revision 2

Thermo-compression of pyrope-grossular garnet solid solutions: non-linear compositional dependence

WEI DU[1, 2], SIMON MARTIN CLARK[3, 4], AND DAVID WALKER[1]

[1]Lamont-Doherty Earth Observatory and Department of Earth and Environmental Sciences, Columbia University in the City of New York, Palisades, New York 10964. USA

[2]Present address: Geodynamic Research Center, Ehime University, Matsuyama 790-8577, Japan

Earth-Life Science Institute, Tokyo Institute of Technology, Tokyo 152-8550, Japan

[3] Department of Earth and Planetary Sciences, Macquarie University, North Ryde, NSW 2109, Australia.

[4]The Bragg Institute, Australian Nuclear Science and Technology Organization, Locked Bag 2001, Kirrawee DC, NSW 2232, Australia.

ABSTRACT

Unit cell parameters of a series of synthetic garnets with the pyrope, grossular, and four intermediate compositions were measured up to about 900K and to 10 GPa using synchrotron X-ray powder diffraction. Coefficients of thermal expansion of pyrope-grossular garnets are in the range 2.10~ 2.74 x 10^{-5} K^{-1} and uniformly increase with temperature. Values for the two end members pyrope and grossular are identical within experimental error 2.74±0.05 x 10^{-5} K^{-1} and 2.73±0.01 x 10^{-5} K^{-1} respectively. Coefficients of thermal expansion for intermediate compositions are smaller than those of end members, and are not linearly dependent on composition. Bulk modulus of grossular is K_0=164.3(1) GPa (with K_0' *the pressure derivative of the bulk modulus* fixed to 5.92) and bulk modulus of pyrope is K_0=169.2(2) GPa (with K_0' fixed to 4.4) using a third order Birch-Murnaghan equation of state, which are consistent with

previously reported values. The bulk moduli of garnets of intermediate composition are between ~155 and ~160 GPa, smaller than those of the end-members no matter which K_0' is chosen. The compositional dependence of bulk modulus resembles the compositional dependence of thermal expansion. Intermediate garnets on this binary have large positive excess volume, which makes them more compressible. We find that excess volumes in the pyrope-grossular series remain relatively large even at high pressure (~6GPa) and temperature (~800K), supporting the observation of crystal exsolution on this garnet join. The curiously "W"-shaped compositional variation of thermal expansion and bulk modulus is anti-correlated with the compositional dependence of microstrain documented in our companion paper (Du et al. in preparation) on the excess volumes in this series of garnets. Minimum thermal expansions and bulk moduli go with maximum microstrains.

Keywords: Pyrope-grossular garnet solid solution, thermal expansion, compressibility, excess volume

INTRODUCTION

Garnets have the general chemical composition $A_3B_2(SiO_4)_3$ where A and B are 2+ and 3+ cations respectively. In nature garnets predominately exist as solid solutions between the following six end member minerals: pyrope ($Mg_3Al_2Si_3O_{12}$), grossular ($Ca_3Al_2Si_3O_{12}$), almandine ($Fe_3Al_2Si_3O_{12}$), spessartite ($Mn_3Al_2Si_3O_{12}$), uvarovite ($Ca_3Cr_2Si_3O_{12}$), and andradite ($Ca_3Fe_2Si_3O_{12}$). Garnet is a major phase in Earth mantle models such as pyrolite and piclogite (Irifune and Ringwood 1987, 1993) and garnet volume fraction may increase to more than 40% in the Earth's transition zone (410-660km) (Duffy and Anderson 1989). They are stable over a wide pressure and temperature range and compatible with phases such as mica, pyroxene, and olivine, making them important candidates for geothermal barometers and thermometers.

Knowledge of the effect of compositional change on the elastic properties of garnet is essential for the correct interpretation of regional lateral variations in seismic velocity imaged by seismic tomography and geodynamic studies of the continental lithosphere in terms of thermal and chemical properties. Least squares techniques might succeed in inverting the elastic properties of natural solid solution samples based on interpolation of end member properties if those elastic properties were strictly linear in compositional dependence or if there is sufficient compositional coverage to resolve some more complex dependence.

Substitution for magnesium by calcium along the pyrope-grossular join involves a large change in cation size and might produce a large change in thermoelastic properties. The mixing volumes and enthalpies of solid solutions of several synthetic and natural garnets along this join have been determined experimentally at ambient temperature and pressure (Newton et al. 1977; Geiger et al. 1987; Wood 1988; Ganguly et al. 1993; Bosenick et al. 1995, 1996, and 1997; Geiger and Feenstra 1997). These previous studies all show that garnet solid solutions on this binary have large positive excess mixing volumes. There have been many measurements of the compressibility and thermal expansion of the end member garnets (Hazen and Finger 1978; Bass 1986; O'Neill et al. 1989; Olijnyk et al. 1991; Gillet et al. 1992; Zhang et al. 1998, 1999; Conrad et al. 1999; Zou et al. 2012), and a few measurements for their solid solutions (Babuska et al. 1987; Bosenick and Geiger 1997). So far there has been no reported measurement of compressibility along the pyrope-grossular join. There has been one measurement of thermal expansion made at low temperature (Bosenick and Geiger 1997), but the data they reported for end member compositions did not agree well with previous study by Skinner (1956).

In this paper, we present the unit cell volumes of pyrope, grossular and garnets with four intermediate compositions to ~900K and ~10GPa. We calculate thermal expansion coefficients

and bulk moduli from these data, and compare our results for the end member compositions to those reported in previous studies. Both thermal expansion and bulk moduli show nonlinear compositional dependence and closely correlate with the non-ideal mixing volume on this join. These new data extend our understanding of the thermoelasticity of garnet solid solutions to high pressure and high temperature as a function of Mg-Ca cation substitution.

Our broader objective in this study is to evaluate whether garnets in this solution series are likely to have a stable two-phase region at high pressures and temperatures that may be relevant to the Earth's upper mantle and transition zone. The large excess volume at higher PT condition calculated from bulk modulus and thermal expansion together with the observed larger excess volume of garnet, which will be discussed in a companion paper, strongly encourage the expectation that a 2-phase garnet region should be encountered in the laboratory at less than 100 kbar. Such garnet exsolution has now been observed experimentally, as it would not be if excess volumes were as small as previously reported.

EXPERIMENTAL PROCEDURES

Crystalline garnet samples with six different compositions (pyrope ($Mg_3Al_2Si_3O_{12}$), $Py_{80}Gr_{20}$ ($Mg_{2.4}Ca_{0.6}Al_2Si_3O_{12}$), $Py_{60}Gr_{40}$ ($Mg_{1.8}Ca_{1.2}Al_2Si_3O_{12}$), $Py_{40}Gr_{60}$ ($Mg_{1.2}Ca_{1.8}Al_2Si_3O_{12}$), $Py_{20}Gr_{80}$ ($Mg_{0.6}Ca_{2.4}Al_2Si_3O_{12}$), grossular ($Ca_3Al_2Si_3O_{12}$)) were synthesized from an anhydrous glass starting material in a multi-anvil (MA) high-pressure cell. The garnet glasses were prepared by melting a finely ground mixture of $CaCO_3$, MgO, Al_2O_3, and SiO_2 powders. The magnesia, alumina, and silica were rigorously dehydrated shortly before weighing into the mix. The mixed powders were heated slowly to 1000°C for several hours in a covered Pt crucible to decarbonate the $CaCO_3$. After heating to 1500-1600°C for several hours, the garnet glasses were cooled

rapidly by quenching the Pt crucible in water. The glasses of the six solid solution compositions were checked by both microprobe and optical methods. The compositions of these six glasses agree very well with the targeted initial proportion of oxides (Table 1).

These glass precursors were then held at ~ 6GPa and 1400±2°C in the MA for 0.5 hours to produce the desired crystalline garnets. We found by *in situ* XRD observations at Station 16.4 of the Daresbury, UK Synchrotron Radiation Source that the key to synthesis of phase-pure garnets by this method is to ensure that garnet growth occurs without previous clinopyroxene nucleation, which we found to occur predominantly in the range 700-1100 °C at the same pressure. Description of the Daresbury 16.4 facility can be found in Clark (1996) and the calibration procedures used there were described by Walker et al. (2000, 2002) and Johnson et al. (2001). So it is crucial to ramp the temperature up above 1100°C as rapidly as possible. Annealing at 1400°C ensures reproducible unit cell sizes and ambient excess volumes by resetting the Mg-Ca disordering [to slightly smaller excess volumes] inherited from the glass starting material. Garnet crystals synthesized in MA were checked by both microprobe and XRD methods. The compositions of these garnets are consistent with the starting glasses within the microprobe measurement error (Table 1) and homogeneous within the counting statistics. The clean XRD peaks of these pyrope-grossular garnets indicate that these MA synthetic garnet solid solutions are phase-pure garnet with *Ia-3d* symmetry (Fig.1).

X-ray powder diffraction patterns from our synthesized garnets at a range of temperatures (300 to 900 K) and then a range of pressures (0 to 10 GPa) were collected at the Advanced Light Source, Lawrence Berkeley National Laboratory (ALS) on beamline 12.2.2, in angular dispersive mode using a MAR345 image plate detector (Kunz et al. 2005). Precisely measuring the sample to detector distance is essential for the determination of accurate lattice parameters.

Beamline 12.2.2 has an automated sample positioning system that allows the sample to detector distance to be set for samples contained in complex sample environments to better than 10μm (Clark et al. 2012). Two series of measurements were carried out: first powder diffraction patterns were measured as a function of temperature and then as a function of pressure.

High-temperature data were collected between 300 and 900K in steps of about 70K using a furnace that was specially designed to take advantage of the automated sample positioning system. This consisted of two diamond windows mounted on Invar seats held inside a stainless steel tube mounted inside a nichrome-wound resistance heater. The furnace was designed so that the heating element was as close to the sample as practically possible. Samples were mixed together with sodium chloride powder as a temperature calibration standard and loaded into 120 μm diameter holes drilled in to 60μm thick stainless steel disks. This assembly was then held loosely between the diamond windows in the furnace. The design of this cell ensures that no pressure can be applied to the sample during heating. Enclosing the sample in a furnace minimizes temperature gradients and allows control of the temperature to better than ±1°C. The temperature was monitored and controlled using a feedback loop by a chromel-alumel (type K) thermocouple placed in contact with the metal gasket and as close to the sample as possible. Because the thermocouple cannot be exactly at the point sampled by the x-ray beam, we were concerned that temperature gradients within the sample area induced by radiative losses through the diamond windows might lead to some difference between the thermocouple temperature and the sample temperature. We therefore used the sodium chloride as an internal temperature sensor.

The diffraction patterns were collected from 5° to 30° 2θ. The diffraction images were obtained with λ=0.4959Å (calculated from energy 25 keV) and the distance between sample and the detector ~440mm was determined for each run through collection of a standard LaB_6

diffraction pattern. In order to collect clear XRD patterns, exposure time was as long as 5 minutes and temperature readings before and after XRD data collection were recorded. The difference between them is not larger than 2°C. Powder diffraction patterns were collected for the garnet sample containing the sodium chloride internal standard at each temperature. The unit cell volume of the sodium chloride was used to calculate the temperature from the thermal part of the BE-2 equation of state of sodium chloride (Birch 1986). We found that as the temperature of the sample increased, the difference between the temperature given by the thermocouple and that from the sodium chloride also increased. The difference is given by the following equation:

$$T_2 = -3.6E - 5 * T_1^2 + 0.982 * T_1 - 0.565 \quad (1)$$

where T_1 (°C) is the K thermocouple temperature and T_2 (°C) is calculated temperature from the EOS of internal standard NaCl. At about 900 K, the temperature reading from thermocouple (T_1) was about 25 °C higher than that calculated from the sodium chloride (T_2), and this discrepancy is an order of magnitude larger than any probable measurement error. Therefore, we used the temperatures given by the sodium chloride (T_2) throughout this work. Thermal expansion of the garnets samples was then calculated based on the unit cell parameters measured at temperatures between 300 and 900 K.

A four-screw symmetric DAC was used for the compressibility measurements. High pressures were generated by applying force with these 4 drive screws onto the small area of the tips of two opposed diamond anvils. The polycrystalline garnet samples were loaded into stainless steel gaskets produced as described above together with one or two ruby chips and a 4:1 mixture of methanol: ethanol which acted as a pressure transmitting medium. This stainless steel gasket serves two purposes: it keeps the diamonds from crushing the crystals and it allows us to surround the crystal with this fluid pressure medium that provides hydrostatic conditions for the

crystals. Pressure determination was performed by measuring the ruby fluorescence shift (Mao et al. 1986) excited by an Ar laser. Pressure values measured before and after each XRD data collection were almost equivalent to each other, the difference being no more than 0.2GPa, and the average value was taken as the pressure of the sample during the unit cell measurements with an error bar of 0.2GPa. At the end of each depressurization process, the unit cell parameter under ambient conditions was measured to give a zero pressure value.

FIT2D software package was used to integrate the two-dimension diffraction rings into one-dimensional diffraction patterns (Hammersley et al. 1996). Since the garnet sample and internal standard peaks were not overlapped, single peak fitting was the most appropriate method for determining the peak positions. The program XFIT (Cheary and Coelho 1996) was used to do this. Once the peak positions were determined for each diffraction pattern, the program REFCEL (Cockcroft and Barnes 1997) was used to refine the unit cell parameters through least squares analysis of the fitting positions of the peaks.

RESULTS AND DATA ANALYSIS

Thermal expansion of pyrope, grossular and the solid solutions

The volume changes with temperature for the six garnet compositions are presented in Table 2 and Figure 2. The volume of garnet on the join pyrope-grossular increases with temperature systematically. We found that a second order polynomial equation fitted our measured volume data for each of these six garnet compositions (Fig. 2). Thermal expansion coefficients, α, for all six garnet compositions were then calculated from the following expression:

$$\alpha(T) = \frac{1}{V_{(T)}}\left(\frac{\partial V}{\partial T}\right)_P \quad (2)$$

where $V_{(T)}$ is taken as the measured unit cell volume at temperature T. For example, thermal

expansion at 300 K is the temperature derivative of the unit cell volume calculated from the fitted polynomial equation divided by the measured unit cell volume at 300K.

The thermal expansion coefficients of the pyrope-grossular garnet solid solution increase with temperature but the compositional dependence at ambient conditions is not monotonic (Table 2 and Fig. 3). The unit cell volume and calculated thermal expansion from Eq. (2) of our MA synthesized end members show consistency with previous studies, yielding $\alpha = 2.74(5) \times 10^{-5}$ K^{-1} for pyrope with a unit cell volume 1502.8(4) $Å^3$; $\alpha = 2.73(1) \times 10^{-5}$ K^{-1} for grossular with a unit cell volume 1664.2(2) $Å^3$, which agrees with previous studies (Bosenick and Geiger 1997; Grêaux et al. 2011; and Zou et al. 2012) (Table 3). Garnets with intermediate composition show smaller thermal expansion than the two end members at ambient condition; and the thermal expansions of garnets with compositions near the end members ($Py_{80}Gr_{20}$, $Py_{20}Gr_{80}$) show relatively smaller thermal expansions than garnets with composition more central to the solution series ($Py_{60}Gr_{40}$, $Py_{40}Gr_{60}$). Normalized volume ($V_T/V_{273.15}$) gives rough estimates of the temperature dependence of thermal expansion for different compositions. We see that the normalized volumes of end members pyrope and grossular increase faster with temperature than the garnet solid solutions with intermediate composition; and among all the garnets with intermediate composition, the normalized volume of $Py_{40}Gr_{60}$ shows the smallest temperature dependence (Fig. 4).

The agreement on unit cell volume and thermal expansions for end-members from different groups suggests that we did not experience any systematic cell measurement problems, therefore, the thermal expansion coefficients of garnet solid solutions with intermediate composition we present in this paper are also reliable and carry very important information for discussing thermal properties of garnet structure. Moreover, with the exception of Gr90, our nonmonotonic

compositional dependence of the high temperature thermal expansions quite closely tracks the low temperature thermal expansions of Bosenick and Geiger (1997) when compared at the temperature of overlap, 300 K. This suggests that the complex thermal expansion dependence on composition shown by both studies may be more than noise.

Different groups have used different numerical equations to describe molar volume changes with respect to temperature, and there is some uncertainty in the calculated thermal expansion coefficient of garnet caused by using these different numerical methods (Skinner 1956; Bosenick and Geiger 1997). Therefore, for our comparison we took the unit cell parameters of pyrope and grossular measured at lower temperature to about 25 K from Bosenick and Geiger (1997), and fitted all the unit cell volume data set with a second order polynomial equation as we did for our own MA synthesized garnets. We find the non-linear volume thermal expansion from our MA synthesized garnets is remarkably consistent in detail with those from Bosenick and Geiger (1997): garnets with intermediate compositions having smaller thermal expansion than the two end-members. Furthermore, garnet solid solution with larger excess volume (composition close to $Py_{50}Gr_{50}$) shows relatively larger thermal expansion than the other intermediate compositions, which shows a similar compositional dependence with isothermal bulk moduli of garnet solid solution on this join as discussed later in this paper.

Compressibility of pyrope-grossular solid solutions

Use of a hydrostatic pressure transmitting medium is important in high pressure experiments. Non-hydrostatic stress propagated by frozen or crystallized pressure-transmitting medium at extreme pressures will affect the measurement of the elastic properties of the samples, including the bulk modulus. Therefore, in order to keep a hydrostatic condition for garnet sample during

high pressure measurements, we do not increase pressure higher than 10GPa, the freezing pressure of the 4:1 mixture of the methanol: ethanol medium (Eggert et al. 1992).

The volume changes with pressure of the six garnet compositions are presented in Figure 5, which shows that with increasing pressure, the volumes of garnets on the join pyrope-grossular decrease systematically. Bulk moduli of garnets on this join were calculated by fitting a third order Birch-Murnaghan EOS (Birch 1986) to these data.

Birch-Murnaghan equation of State

In the case of isothermal hydrostatic compression, the pressure can be written with BE_2 form (Birch 1986):

$$P_i = 3K_0 f(1+2f)^{\frac{5}{2}}(1+Af+Bf^2) \quad (3)$$

Here, f is the Eulerian strain, with sign reversed so f is positive for compression $f = \frac{1}{2}\left[\left(\frac{V}{V_0}\right)^{-\frac{2}{3}} - 1\right]$ and $A = \frac{3}{2}(K_0' - 4)$; the isothermal EOS for cubic symmetry samples such as pyrope-grossular garnets can be obtained as BE_1 by setting B=0 in form BE_2. V_0 is the volume at P=0; K_0 is isothermal bulk modulus at zero pressure and K_0' is its first derivative of K versus pressure at P=0. In this study, the upper limit of the pressure during compression is ~10 GPa, which may still not be high enough to allow a precise calculation of K_0' because compressions of only about 5% was achieved in 10 GPa (Angel 2000).

Numerous studies of elastic properties using X-ray diffraction techniques (Hazen and Finger 1989; Olijnyk et al. 1991; Zhang et al. 1998, 1999; Pavese et al. 2001; Grêaux et al. 2011; Zou et al. 2012) and ultrasonic interferometry (Gwanmesia et al. 2006) or resonant ultrasound spectroscopy as well as light scattering methods such as Brillouin spectroscopy (Conrad et al. 1999; Sinogeikin and Bass 2000; Jiang et al. 2004) have been performed at ambient and high pressure on garnet end-members. There is good agreement for elastic properties (K_0) of these

end-members among various studies at ambient conditions, although the pressure derivative of the bulk modulus (K_0') for end-members of garnet ranges from 4.0 to 6.1, and are less consistent (Table 5).

The P-V curve of grossular of up to about 37 GPa allowed a good estimate of the first pressure derivative of the bulk modulus (K_0'=5.92) (Pavese et al. 2001). Since our low-pressure P-V data (~ 7 GPa) are consistent with theirs, we calculated K_0 by fitting the measured P-V data to EOS with K_0'=5.92, which gave K_0=164.3(1) GPa for the bulk modulus of grossular. The extrapolation of P-V value based on Birch-Murnaghan EOS and K_0=164.3(1) GPa, K_0'= 5.92 is in better agreement with those measured P-V from Pavese et al. (2001) experiment compared with extrapolation with K_0'= 4.4 (Fig. 6). In addition, the calculated K value of grossular synthesized in MA is also in good agreement with the theoretically calculated value K_0=166 GPa (Akhmatskaya et al. 1999), Brillouin scattering result K_0=165.68 GPa, K_0'=5.46 (Conrad et al. 1999), and most recently result K_0=166 GPa from Grêaux et al. (2011).

In garnet structure, the dodecahedral cations Ca^{2+} and Mg^{2+} have a mean ionic radii of 1.26 and 1.03 Å (Shannon 1976), respectively, and are thus near the upper and lower limits for the X-cation size. The substitution between Ca^{2+} and Mg^{2+} in the dodecahedral X site may be an influential factor in K_0' (the first derivative of bulk modulus) (Conrad et al. 1999), therefore, we expect the K_0' might be different for pyrope and grossular garnets. Our P-V data of pyrope garnet is consistent with those reported by Zhang et al. (1998) using He as pressure transmitting medium and successfully keeping their pyrope samples in hydrostatic condition until pressure about 30 GPa (Fig. 6). The fit of our pyrope P-V data to EOS with fixed K_0'=4.4 (Zhang et al. 1998) yield K_0=169.2(2) GPa, in agreement with those previously reported. The extrapolations of P-V value of pyrope based on the Birch EOS with K_0'=4.4, K_0=169.2 GPa and K_0'=5.92,

K_0=164.1 GPa, respectively, are also showed in Figure 6, and the extrapolation with K_0'=4.4 and K_0=169.2 GPa agrees better with Zhang et al. (1999) high-pressure P-V measurements.

There is no previous high-pressure data to constrain the K_0' values for garnets with intermediate compositions on the join pyrope-grossular. Since our end member data also confirm that the substitution of the dodecahedral cation Ca^{2+} for Mg^{2+} in the garnet structure decreases K_0 and increases K_0', we calculated the bulk moduli of garnet solid solution by using Birch-Murnaghan EOS with two different fixed K_0' values. Our fitting results show that with a fixed K_0' value, there is no large difference in bulk moduli for garnet with intermediate composition; they are all about 155 GPa by fixing K_0'=5.92 or about 160 GPa by fixing K_0'=4.4. There is a weak nonmonotonic compositional dependence that is reminiscent of the nonmonotonic thermal expansion dependence on composition seen in Figure 3 (Table 6, Fig. 7). However, the intermediate composition compressibilities are all relatively smaller than those of the end members, no matter what K_0' value was chosen to fit in the Birch-Murnaghan EOS.

DISCUSSION AND IMPLICATION

Our new synchrotron X-ray diffraction data on pyrope-grossular solid solution show that substitution of Mg^{2+} for Ca^{2+} along the pyrope-grossular join produces changes in thermoelastic properties. Garnets with intermediate composition show smaller thermal expansion and smaller bulk modulus than the two end members.

The relatively smaller bulk modulus of garnet solid solution is consistent with the positive excess volume reported by previous studies (e.g. Ganguly et al. 1993) and confirmed and increased in our companion study (Du et al. in preparation). Positive excess volume of garnets with intermediate composition makes them more compressible under high pressure, which is consistent with the relatively smaller calculated K_0. If the positive excess volumes are comprised

of defects or local strains in the lattice accommodating Ca-Mg size mismatches by incorporating void space around Mg cations, then the greater compressibility reflects the greater compliance of the intermediate composition structures with extra mismatch room. Although more information about the distribution of Mg and Ca cations depends on further research, we do notice the similarity of the compositional dependence of thermal expansion and bulk modulus (Figs. 3 and 7). Garnets with composition close to the end members show smaller thermal expansion and smaller bulk modulus compared with those on the middle of pyrope-grossular join. We observed that microstrain values calculated from XRD peak width (Du et al. in preparation) show correlation with the thermal expansion and bulk modulus. And XRD profiles analysis of these garnets (e.g. $Py_{80}Gr_{20}$) shows that these garnets carry more microstrain than those with composition close to the middle of this join ($Py_{40}Gr_{60}$). The different microstrain values along pyrope-grossular join could be a reflection of different degree of short range ordering of Ca and Mg achieved through high-pressure synthesis. Further results on microstrain and Mg-Ca ordering are reported in our companion paper.

The calculation of the thermal expansion coefficient in this paper was based on the assumption that a quadratic equation is good enough to describe the unit cell volume of garnet as it changes with temperature. But it is doubtful whether this dependence can be extrapolated to temperatures in excess of 1300K where additional interesting garnet petrogenesis occurs. We are limited at present to temperatures of 800 K for the excess mixing volume on this join, which is shown in Figure 8. Pyrope-grossular solid solutions show large positive excess volume at all conditions so far measured; this excess volume on the pyrope-grossular join decreases with temperature, but still does not vanish even at 800 K.

Excess volumes of pyrope-grossular garnets at 6 GPa were calculated by applying the bulk

moduli to the Birch-Murnaghan EOS (with K_0' fixed to 5.92), and are also presented in Figure 8. Excess volumes on the pyrope-grossular join decrease systematically with pressure, and positive unit cell excess volume values as large as 10Å^3/cell for garnet with a composition of $Py_{40}Gr_{60}$ persist at pressures as high as 6 GPa. Combined with the high temperature results calculated from thermal expansion coefficients, significant positive excess volumes persists as temperature and pressure increase, suggesting that phase exsolution at high pressure and high temperature should be observable. We confirm experimentally that such exsolution is observed. For example, two garnets with different composition along pyrope-grossular join were chosen as starting material, and heated at 8GPa and 1200°C for ~20 days. Quenched samples from these annealing experiments were checked by XRD scan, and both composition convergence and divergence were observed. Details about the phase separation experiments on pyrope-grossular join will be discussed in our companion paper.

ACKNOWLEDGMENTS

This work was supported by the U.S. National Science Foundation. The Advanced Light Source is supported by the Director, Office of Science, Office of Basic Energy Sciences, of the U.S. Department of Energy under Contract No. DE-AC02-05CH11231 at Lawrence Berkeley National Laboratory. We thank Jean Hanley, Jinyuan Yan, Geoff Whelan and Raj Dasgupta for their technical assistance.

REFERENCES CITED

Angel, R.J. (2000) Equations of state. In: Hazen, R.M. and Downs, R.T., Editors, High-pressure and high-temperature crystal chemistry. Reviews in Mineralogy and Geochemistry, 41, 35-60.

Akhmatskaya, E.V., Nobes, R.H., Milman, V., and Winkler, B. (1999) Structural properties of garnets under pressure : An ab initio study. Zeitschrift für Kristallographie, 214, 808-819.

Babuska, V., Fiala, J., Kumazawa, M., Ohno, I., and Sumino, Y. (1978) Elastic properties of garnet solid-solution series. Physics of The Earth and Planetary Interiors, 16(2), 157-176.

Bass, J. (1986) Elasticity of uvarovite and andradite garnets. Journal of Geophysical Research, 91, 7505-7516.

Birch, F. (1986) Equation of State and Thermodynamic Parameters of NaCl to 300 kbar in the High-Temperature Domain. Journal of Geophysical Research, 91, 4949-4954.

Bosenick, A., and Geiger, C.A. (1997) Powder X-ray diffraction study of synthetic pyrope-grossular garnets between 20 and 295 K. Journal of Geophysical Research, 102, 22649-22657.

Bosenick, A., Geiger, C.A., and Cemic, L. (1996) Heat capacity measurements of synthetic pyrope-grossular garnets between 320 and 1000 K by differential scanning calorimetry. Geochimica et Cosmochimica Acta, 60(17), 3215-3227.

Bosenick, A., Geiger, C.A., Schaller, T., and Sebald, A. (1995) A ^{29}Si MAS NMR and IR spectroscopic investigation of synthetic pyrope-grossular garnet solid solutions. American Mineralogist, 80, 691-704.

Cheary, R.W., and Coelho, A.A. (1996) Programs XFIT and FOURYA, deposited in CCP14 powder diffraction library. Engineering and Physical Sciences Research Council, Daresbury Laboratory, Warrington, England.

Clark, S.M. (1996) A new energy dispersive powder diffraction facility at the SRS. Nuclear Instruments and Methods in Physics Research, A381, 161-168.

Clark, S.M., MacDowell, A.A., Knight, j., Kalkan, B., Yan, J., Chen, B., and Williams, Q. (2012) Beamline 12.2.2: An extreme conditions beamline at the Advanced Light Souce. Technical Reports, 25, 10-11.

Conrad, P.G., Zha, C.S., Mao, H.K., and Hemley, R.J. (1999) The high-pressure, single-crystal elasticity of pyrope, grossular, and andradite. American Mineralogist, 84, 374-383.

Cockcroft, J.K., and Barnes, P. (1997) Powder diffraction on the web, originally an internet-based advanced certificate course offered by Birkbeck College, but with the static course material since released on the group's web site: http://pd.chem.ucl.ac.uk/pd/welcome.htm.

Duffy, T.S., and Anderson, D.L. (1989) Seismic velocities in mantle minerals and the mineralogy of the upper mantle. Journal of Geophysical Research, 94, 1895–1912.

Eggert, J.H., Xu, L.W., Che, R.Z., Chen, L.C., and Wang, J.F. (1992) High pressure refractive index measurements of 4:1 methanol:ethanol. Journal of Applied Physics, 72, 2453-2461.

Ganguly, J., Cheng, W.J., and O'Nell, H.S. (1993) Syntheses, volume, and structural changes of garnets in the pyrope-grossular join: Implications for stability and mixing properties. American Mineralogist, 78, 583-593.

Geiger, C.A., and Feenstra, A. (1997) Molar volumes of mixing of almandine-pyrope and almandine-spessartine garnets and the crystal chemistry and thermodynamic-mixing properties of the aluminosilicate garnets. American Mineralogist, 82, 571-581.

Geiger, C.A., Newton, R.C., and Kleppa, O.J. (1987) Enthalpy of mixing of synthetic almandine-grossular and almandine-pyrope garnets from high-temperature solution calorimetry. Geochimica et Cosmochimica Acta , 51(6), 1755-1763.

Gillet, P., Fiquet, G., Malezieux, J.M., and Geiger, C.A. (1992) High-pressure and high-temperature Raman spectroscopy of end-member garnets: pyrope, grossular and andradite. European Journal of Mineralogy, 4, 651-664.

Gwanmesia, G.D., Zhang, J.Z., Darling, K., Kung, J., Li, B.S., Wang, L.P., Neuville, D., and Liebermann, R.C. (2006) Elasticity of polycrystalline pyrope ($Mg_3Al_2Si_3O_{12}$) to 9 GPa and 1000 °C. Physics of the Earth and Planetary Interiors, 155, 179-190.

Hammersley, A.P., Svensson, S.O., Hanfland, M., Fitch A.N., and Häusermann, D. (1996) Two-Dimensional detector software: from real detector to idealised image or two-theta scan. High Pressure Research, 14, 235-248.

Hazen, R.M., and Finger, L.W. (1978) Crystal structures and compressibilities of pyrope and grossular to 60kbar. American Mineralogist, 63, 297-303.

Hazen, R.M., and Finger, L.W. (1989) High pressure crystal chemistry of andradite and pyrope: revised procedures for high pressure diffraction experiments. American Mineralogist, 74, 352-359.

Irifune, T., and Ringwood, A.E. (1987) Phase transformation in primitive MORB and pyrolite compositions to 25 GPa and some geophysical implications. In: Manghnani, M.H. and Syono, Y., Editors, High pressure research in mineral physics. vol. 39, TERRAPUB Tokyo/American Geophysical Union, Washington, DC: 235-246.

Irifune, T., and Ringwood, A.E. (1993) Phase transformations in subducted oceanic crust and buoyancy relationships at depths of 600-800 km in the mantle. Earth and Planetary Science Letters, 117(1-2), 101-110.

Jiang, F., Speziale, S., and Duffy, T.S. (2004) Single-crystal elasticity of grossular- and almandine-rich garnets to 11 GPa by Brillouin scattering. Journal of Geophysical Research, 109, 1-10.

Kunz, M., MacDowell, A.A., Caldwell, W.A., Cambie, D., Celestre, R.S., Domning, E.E., Duarte, R.M., Gleason, A.E., Glossinger, J.M., Kelez, N., Plate, D.W., Yu, T., Zaug, J.M., Padmore, H.A., Jeanloz, R., Alivisatos, A.P., Clark S.M. (2005) A beamline for high-pressure studies at the Advanced Light Source with a superconducting bending magnet as the source. Journal of synchrotron radiation, 12, 650-658.

Mao, H.K., Xu, J., and Bell, P.M. (1986) Calibration of the ruby pressure gauge to 800 kbar under quasi-hydrostatic conditions. Journal of Geophysical Research, 91, 4673-4676.

Newton, R.C., Charlu, T.V., and Kleppa, O.J. (1977) Thermochemistry of high pressure garnets and clinopyroxenes in the system CaO-MgO-Al_2O_3-SiO_2. Geochimica et Cosmochimica Acta, 41, 369-377.

Olijnyk, H., Paris, E., Geiger, C.A., and Lager, G.A. (1991) Compressional study of katoite [$Ca_3Al_2(O_4H_4)_3$] and grossular garnet. Journal of Geophysical Research, 96, 14313-14318.

O'Neill, B., Bass, J., Smyth, Joe R., Vaughan, M.T. (1989) Elasticity of a grossular-pyrope-almandine garnet. Journal of Geophysical Research, 94, 17819-17824.

Pavese, A., Levy, D., and Pischedda, V. (2001) Elastic properties of andradite and grossular, by synchrotron X-ray diffraction at high pressure conditions. European Journal of Mineralogy, 13, 929-937.

Shannon, R.D. (1976) Revised effective ionic radii and systematic studies of interatomic distances in halides and chalcogenides. Acta Crystallographica, A32, 751-767.

Sinogeikin, S.V., and Bass, J.D. (2000) Single-crystal elasticity of pyrope and MgO to 20 GPa by Brillouin scattering in the diamond cell. Physics of the Earth and Planetary Interiors, 120, 43-62.

Skinner, B.J. (1956) Physical properties of end-members of garnet group. American Mineralogist, 41, 428-436.

Grêaux S., Kono, Y., Nishiyama, N., Kunimoto, T., Wada, K., and Irifune, T. (2011) P-V-T equation of state of $Ca_3Al_2Si_3O_{12}$ grossular garnet. Physics and Chemistry of Minerals, 38, 85-94.

Walker, D., Clark, S.M., Jones, R.L., and Cranswick, L.M. (2000) Rapid methods for the calibration of solid-state detectors. Journal of Synchrotron Radiation, 7, 18–21.

Walker, D., Cranswick, L.M.D., Verma, P.K., Clark, S.M., and Buhre, S. (2002) Thermal equations of state for B1 and B1 KCl. American Mineralogist, 87, 805–812.

Wood, B.J. (1988) Activity measurements and excess entropy-volume relationships for pyrope-grossular garnets. Journal of Geology, 96, 721-729.

Zhang, L., Ahsbahs, H., and Kutoglu, A. (1998) Hydrostatic compression and crystal structure of pyrope to 33GPa. Physics and Chemistry of Minerals, 25, 301-307.

Zhang, L., Ahsbahs, H., Kutoglu, A., and Geiger, C.A. (1999) Single-crystal hydrostatic compression of synthetic pyrope, almandine, spessartine, grossular and andradite garnets at high pressures. Physics and Chemistry of Minerals, 27, 52-58.

Zou, Y.T., Grêaux S., Irifune, T., Whitaker, M.L., Shinmei, T., and Higo, Y. (2012) Thermal equation of state of $Mg_3Al_2Si_3O_{12}$ pyrope garnet up to 19 GPa and 1,700K. Physics and Chemistry of Minerals, 39, 589-598.

FIGURE 1. X-ray profiles of the synthetic pyrope-grossular garnets at ambient conditions. X-ray diffraction scans were collected at the ALS, Lawrence Berkeley National Laboratory on beamline 12.2.2, in angular dispersive mode with λ=0.4959Å (25 keV).

FIGURE 2. Unit cell volumes of pyrope-grossular garnet at ambient pressure with temperature from 300 to about 900 K. Error bars are not apparent because they are smaller than the marker symbols.

FIGURE 3. Thermal expansion coefficients of pyrope-grossular garnet solid solution at ambient conditions. The thermal expansion of our MA synthesized garnet solid solution calculated from high temperature (300~900K) data shows excellent agreement at 300 K with the 300 K results of the previous study of Bosenick and Geiger (1997) calculated from low temperature 20-300K data, with the exception of Gr_{90}. Error bars are calculated from esd of garnet unit cell parameters.

FIGURE 4. Change of normalized unit cell volume as a function of temperature for pyrope, grossular, and four intermediate compositions.

FIGURE 5. Unit cell volume of pyrope-grossular garnets decrease systematically with pressure up to ~10GPa. Error bars are not apparent because they are smaller than the marker symbols.

FIGURE 6. Volume of grossular and pyrope under high pressure calculated by fixing K'=5.92 and K'=4.4. For grossular, extrapolations of unit cell volume to higher pressure with K'=5.92

agree well with experiment result from Pavese et al. (2001); for pyrope, calculated unit cell volumes agree well with Zhang et al. (1998) with K'=4.4.

FIGURE 7. Bulk moduli of garnet solid solution calculated by fixing K'=5.92 and 4.4. Pyrope has larger bulk modulus than grossular, and garnets with intermediate composition on pyrope-grossular join have much smaller bulk moduli than the end-members.

FIGURE 8. Positive excess volumes of garnets synthesized by using multi-anvil (MA) techniques at LDEO at high temperature and high pressure, which are larger than previous studies on garnets synthesized by using piston cylinder (PC) (e.g. Ganguly et al. 1993). The excess volumes on this join decrease with temperature and pressure, but still remain at a significant level at 770K or 6GPa.

TABLE 1. Microprobe analyses of starting glasses and corresponding MA garnets synthesized from those glasses (averaged compositions for 10 analyses in wt. %) and their calculated Ca/(Mg+Ca) atomic ratio.

Molecular Formula	MgO	CaO	SiO_2	Al_2O_3	Sum	Ca/(Ca+Mg)
Pyrope(glass)	31.21	0.04	44.53	25.19	100.97	0
Pyrope(crystal)	31.58	0.05	44.08	25.00	100.71	0
$Py_{80}Gr_{20}$ (glass)	23.22	8.40	44.00	24.63	100.26	0.206
$Py_{80}Gr_{20}$ (crystal)	23.04	8.54	45.26	24.08	100.91	0.210
$Py_{60}Gr_{40}$ (glass)	17.55	16.46	41.86	24.02	99.99	0.403
$Py_{60}Gr_{40}$ (crystal)	17.74	16.66	41.95	23.93	100.27	0.403
$Py_{40}Gr_{60}$ (glass)	11.69	24.21	40.78	23.61	100.29	0.598
$Py_{40}Gr_{60}$ (crystal)	11.69	24.80	40.21	23.30	100.00	0.603
$Py_{20}Gr_{80}$(glass)	5.56	31.64	40.19	22.26	99.66	0.804
$Py_{20}Gr_{80}$ (crystal)	5.60	32.05	40.08	22.85	100.58	0.805
Grossular (glass)	0.01	37.76	39.13	22.31	99.22	1
Grossular (crystal)	0.01	37.83	39.17	22.28	99.29	1

TABLE 2. The unit cell volume and thermal expansion of pyrope-grossular. *

Composition	T(K)	a (Å)	Vcell($Å^3$)	$\alpha*10^5(K^{-1})$
Pyrope	294.4	11.4543(11)	1502.8(4)	2.741(52)
	365.2	11.4633(8)	1506.3(3)	2.824(34)
	416.7	11.4685(9)	1508.4(3)	2.886(21)
	462.5	11.4729(9)	1510.1(3)	2.941(8)
	509.8	11.4781(10)	1512.2(4)	2.997(16)
	557.4	11.4836(7)	1514.4(3)	3.053(28)
	605.3	11.4891(10)	1516.6(4)	3.109(46)
	672.2	11.4990(11)	1520.5(4)	3.186(46)
	750.7	11.5071(11)	1523.7(4)	3.278(60)
	295.3	11.4552(9)	1503.2(4)	2.637(11)
	332.5	11.4602(9)	1505.1(4)	2.702(7)
	390.4	11.4649(10)	1507.0(4)	2.806(1)
	434.9	11.4713(11)	1509.5(4)	2.883(6)
	481.0	11.4745(9)	1510.8(4)	2.966(12)
	525.0	11.4808(10)	1513.3(4)	3.042(18)
	575.6	11.4869(7)	1515.7(3)	3.130(24)
	638.2	11.4937(7)	1518.4(3)	3.240(32)
	698.5	11.5025(8)	1521.9(3)	3.343(39)

	738.3	11.5066(7)	1523.5(3)	3.412(45)
$Py_{80}Gr_{20}$	300.0	11.5466(4)	1539.4(2)	2.382(11)
	379.1	11.5543(4)	1542.5(2)	2.487(6)
	451.0	11.5601(4)	1544.8(2)	2.582(2)
	513.8	11.5675(4)	1547.8(2)	2.664(1)
	581.0	11.5741(4)	1550.5(2)	2.752(5)
	645.1	11.5817(4)	1553.5(2)	2.835(9)
	701.2	11.5877(4)	1555.9(2)	2.908(12)
	771.2	11.5951(4)	1558.9(2)	2.998(16)
	837.1	11.6032(6)	1562.2(2)	3.082(20)
$Py_{60}Gr_{40}$	296.1	11.6433(6)	1578.4(2)	2.425(4)
	358.7	11.6497(5)	1581.0(2)	2.521(4)
	409.3	11.6538(5)	1582.7(2)	2.599(4)
	458.7	11.6587(6)	1584.7(2)	2.674(3)
	505.1	11.6636(4)	1586.7(2)	2.744(2)
	559.9	11.6703(6)	1589.5(2)	2.826(1)
	611.7	11.6754(4)	1591.5(2)	2.904(1)
	656.5	11.6822(5)	1594.3(2)	2.97(1)
	710.7	11.6869(6)	1596.2(2)	3.052(1)
	750.5	11.6928(6)	1598.6(2)	3.110(1)
	801.4	11.6977(6)	1600.7(2)	3.186(1)
	842.7	11.7034(5)	1603.0(2)	3.246(1)
$Py_{40}Gr_{60}$	309.8	11.7252(6)	1612.0(2)	2.258(1)
	391.8	11.7330(6)	1615.2(2)	2.364(5)
	458.7	11.7388(5)	1617.6(2)	2.451(1)
	526.3	11.7467(5)	1620.9(2)	2.537(1)
	589.6	11.7522(5)	1623.1(2)	2.619(1)
	652.7	11.7583(6)	1625.7(2)	2.700(1)
	716.4	11.7653(6)	1628.6(2)	2.780(1)
	771.2	11.7710(5)	1630.9(2)	2.850(2)
	831.5	11.7791(6)	1634.3(2)	2.924(3)
$Py_{20}Gr_{80}$	310.8	11.7889(6)	1638.4(2)	2.129(33)
	360.6	11.7934(6)	1640.3(3)	2.232(24)
	428.7	11.7991(5)	1642.7(2)	2.372(12)
	507.0	11.8061(8)	1645.6(3)	2.532(1)

	573.4	11.8138(4)	1648.8(2)	2.667(12)
	643.2	11.8210(7)	1651.8(3)	2.808(24)
	704.0	11.8282(6)	1654.8(2)	2.931(35)
	764.6	11.8351(7)	1657.7(3)	3.052(45)
	802.3	11.8412(5)	1660.3(2)	3.126(51)
	846.5	11.8440(12)	1661.5(5)	3.216(58)
Grossular	296.1	11.8505(4)	1664.2(2)	2.729(4)
	393.7	11.8548(3)	1666.0(1)	2.731(4)
	447.1	11.8602(3)	1668.3(1)	2.733(4)
	501.2	11.8678(4)	1671.5(2)	2.733(4)
	547.4	11.8719(4)	1673.3(2)	2.735(4)
	581.0	11.8762(3)	1675.1(1)	2.735(4)
	584.9	11.8762(5)	1675.1(2)	2.736(5)
	633.6	11.8833(4)	1678.1(2)	2.736(5)
	678.4	11.8881(4)	1680.1(1)	2.737(5)
	727.7	11.8924(3)	1681.9(1)	2.739(5)
	767.5	11.8962(6)	1683.5(3)	2.740(5)
	816.5	11.9008(4)	1685.5(2)	2.742(5)
	859.6	11.9064(4)	1687.9(2)	2.743(5)

* Temperature is calculated from NaCl internal standard with an error bar of 0.2°C. Values in parentheses represent estimated standard deviation through least square fitting for unit cell parameter. Thermal expansion of these garnet solid solutions was calculated with equation (1).

TABLE 3. The unit cell volume and thermal expansion of end members pyrope and grossular at ambient conditions.

	Pyrope		Grossular	
	α (10^{-5} K^{-1})	V_0 (Å^3)	α (10^{-5} K^{-1})	V_0 (Å^3)
Bosenick and Geiger 1997	2.61(3)	1503.2(1)	2.66(2)	1664.4(2)
Grêaux et al. 2011			2.62±0.23	1664(2)
Zou et al. 2012	2.89±0.33	1500(2)		
This study	2.74(5)	1502.8(4)	2.73(1)	1664.2(2)

TABLE 4. The change of unit cell volume of pyrope-grossular with pressure*.

Composition	P(GPa)	a(Å)	Vcell(Å^3)	V (cm^3/mol)
Grossular	0	11.8505 (4)	1664.2(2)	125.23(2)

	1.0	11.8275(5)	1654.5(2)	124.50(2)
	3.2	11.7760(5)	1633.0(2)	122.88(2)
	4.3	11.7523(6)	1623.2(3)	122.15(1)
	6.1	11.7205(5)	1610.1(2)	121.16(1)
	6.8	11.7072(9)	1604.6(4)	120.74(3)
	7.8	11.6911(7)	1598.0(3)	120.25(2)
	9.1	11.6747(5)	1591.2(2)	119.74(2)
$Gr_{80}Py_{20}$	0	11.7857(6)	1637.0(3)	123.19(2)
	1.4	11.7499(7)	1622.2(3)	122.07(2)
	2.9	11.7129(6)	1606.9(3)	120.92(2)
	4.7	11.6756(7)	1591.6(3)	119.77(2)
	6.4	11.6414(6)	1577.6(3)	118.72(2)
	7.7	11.6135(7)	1566.3(3)	117.87(2)
$Gr_{60}Py_{40}$	1.7	11.6858(5)	1595.8(2)	120.08(2)
	2.8	11.6608(4)	1585.6(2)	119.31(2)
	3.9	11.6364(5)	1575.6(2)	118.57(1)
	4.5	11.6247(6)	1570.9(2)	118.21(2)
	5.2	11.6072(7)	1563.8(3)	117.68(2)
	0	11.7262(5)	1612.4(2)	121.33(2)
$Gr_{40}Py_{60}$	0	11.6446(6)	1579.0(2)	118.82( )
	1.4	11.6101(6)	1565.0(2)	117.76(2)
	2.8	11.5770(6)	1551.6(2)	116.76(2)
	4.6	11.5410(6)	1537.2(2)	115.68(1)
	5.7	11.5181(7)	1528.0(3)	114.99(1)
$Gr_{20}Py_{80}$	0	11.5458(4)	1539.1(2)	115.82( )
	1.4	11.5110(5)	1525.3(2)	114.78(1)
	1.5	11.5058(9)	1523.2(4)	114.62(3)
	3.8	11.4589(4)	1504.6(1)	113.22(1)
	5.5	11.4239(5)	1490.9(2)	112.19(1)
Pyrope	0.4	11.4470(6)	1500.0(3)	112.87(2)
	0.7	11.4357(7)	1495.5(3)	112.54(2)
	1.3	11.4245(6)	1491.1(2)	112.21(1)
	2.5	11.3996(8)	1481.4(3)	111.48(2)

	3.8	11.3727(7)	1470.9(3)	110.69(1)
	4.3	11.3608(4)	1466.3(1)	110.34(1)
	5.2	11.3506(4)	1462.4(2)	110.04(2)
	6.5	11.3199(7)	1450.5(3)	109.15(2)
	7.1	11.3091(5)	1446.4(2)	108.84(1)
	0	11.4553(6)	1503.2(2)	113.12(1)

* Pressure is calculated from internal ruby standard with an error bar of 0.1GPa. Values in parentheses represent estimated standard deviation through least square fitting for unit cell parameter.

TABLE 5. Bulk moduli and their first pressure derivative of pyrope and grossular

Isothermal bulk modulus	Method	Pyrope		Grossular	
		K	K'	K	K'
Hazen and Finger. 1989	DAC and XRD	179±3	4*	159±2	4*
Olijnyk et al. 1991	DAC and XRD			168±2.5	6.1±0.15
Conrad et al. 1999	BS	171.32	3.22	165.68	5.46
Akhmatskaya et al. 1999	Theoretically	170	4.2	166	4.3
Zhang et al. 1998	DAC and XRD	171	4.4*	175±1	4.4*
Sinogeikin and Bass 2000	BS	171.2±3	4.1±0.3		
Pavese et al. 2001	DAC and XRD			169.3±1.2	5.92±0.14
Jiang et al. 2004	BS	174.9±1.6	4.7±0.3	169±0.9	3.8±0.2
Gwanmesia et al. 2006	UI	175(2)	3.9(0.3)		
Grêaux et al. 2011	MA and XRD			166	4.04-4.35
Zou et al. 2012	MA and XRD	167±6	4.6±0.3		

*fixed K' number; DAC and XRD, synchrotron radiation powder diffraction on Diamond Anvil Cell; BS, Brillouin scattering; UI, ultrosonic interferometry; MA and XRD, synchrotron radiation powder diffraction on Multi-anvil Device.

TABLE 6. Bulk moduli of pyrope-grossular solid solution.

Composition	Pyrope	$G_{20}P_{80}$	$G_{40}P_{60}$	$G_{60}P_{40}$	$G_{80}P_{20}$	Grossular
K'=4.4	169.2(2)	159.1(2)	161.8(1)	160.7(1)	158.3(1)	169.7(4)
K'=5.92	164.1(2)	156.7(1)	157.9(1)	158.0(1)	153.1(1)	164.3(1)

FIGURE 1.

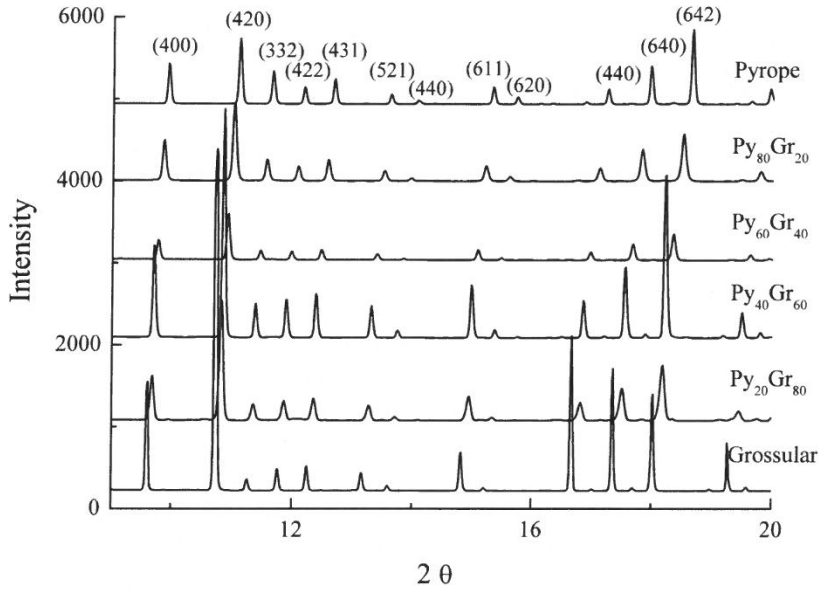

FIGURE 2.

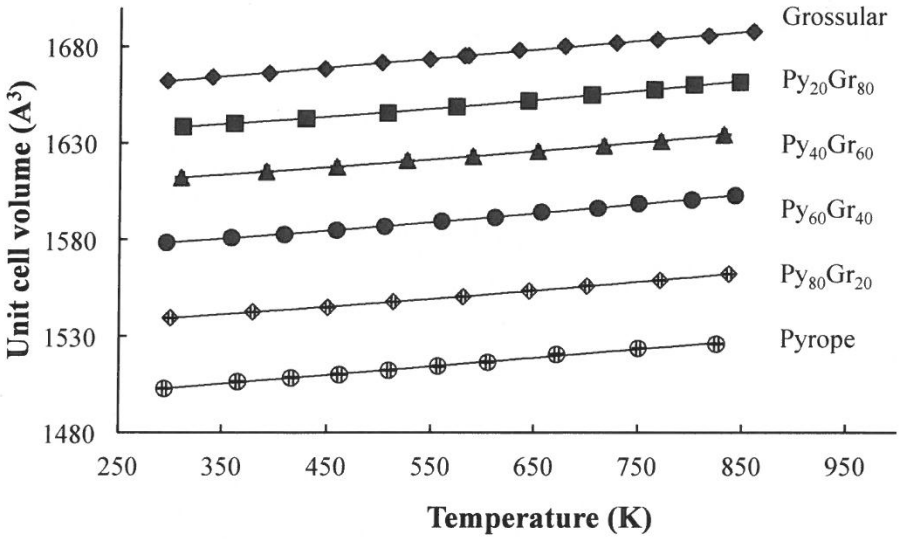

FIGURE 3.

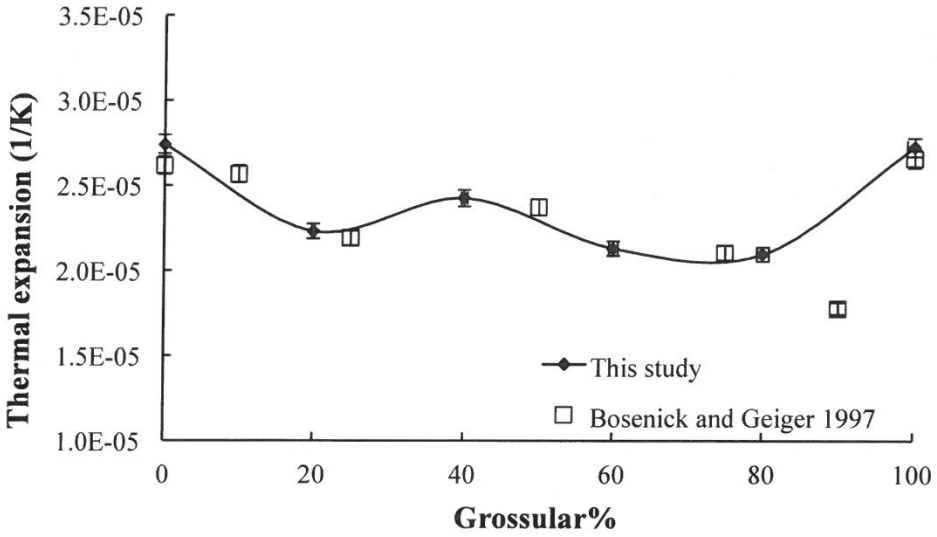

FIGURE 4.

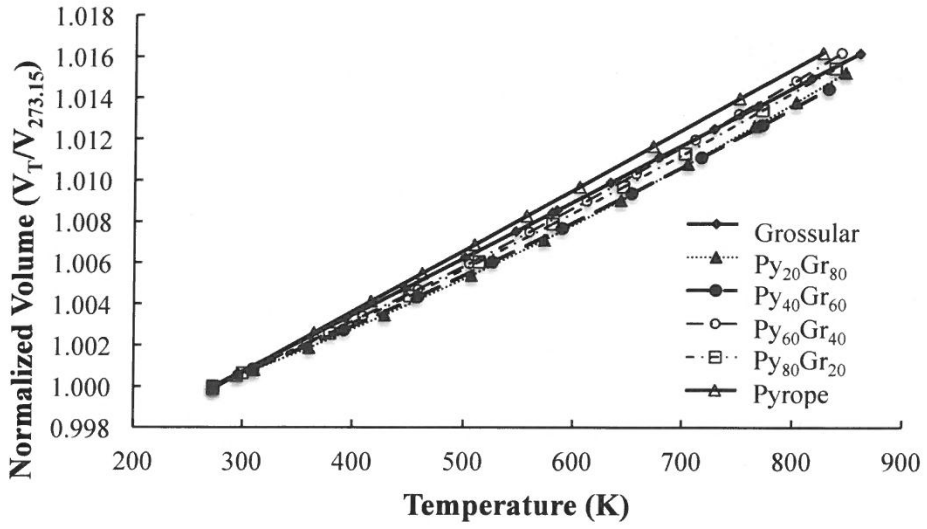

FIGURE 5.

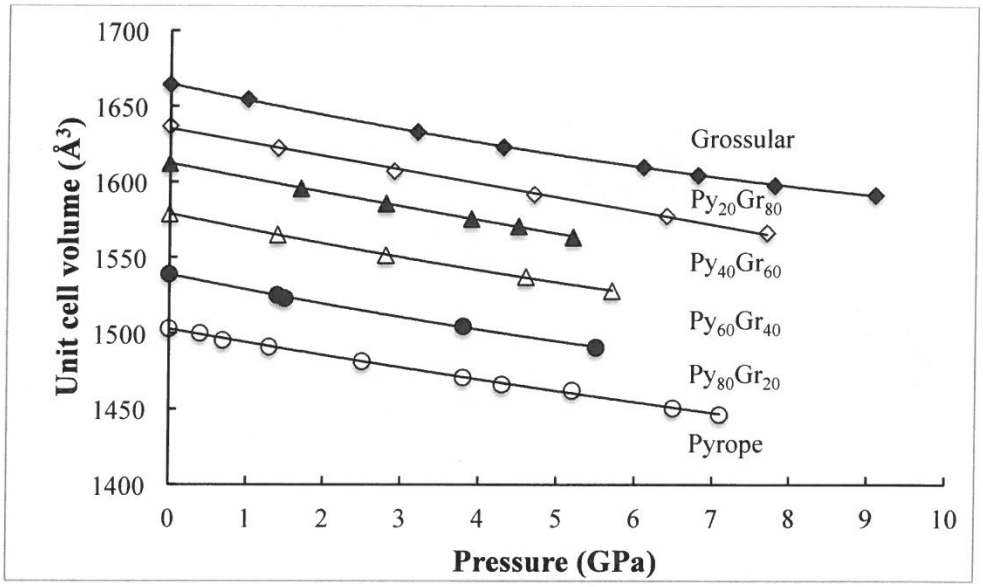

FIGURE 6.

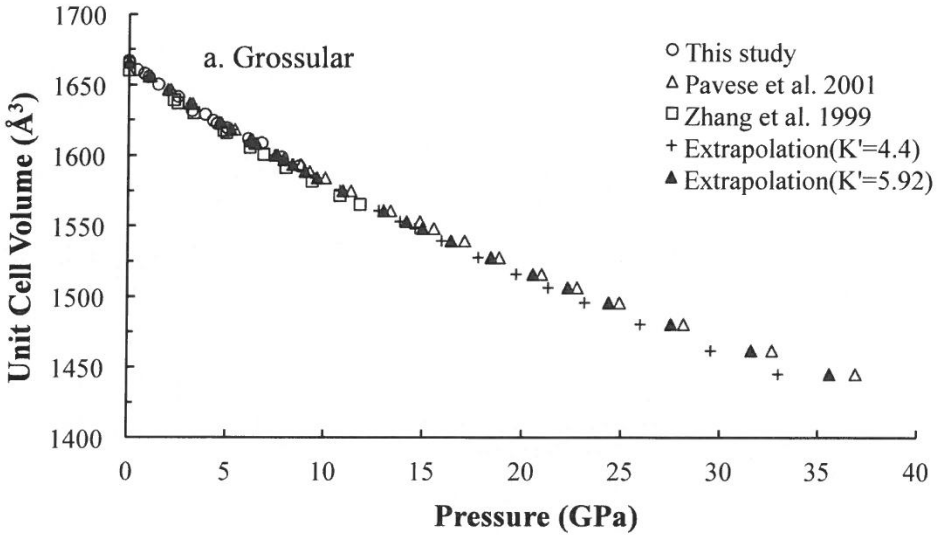

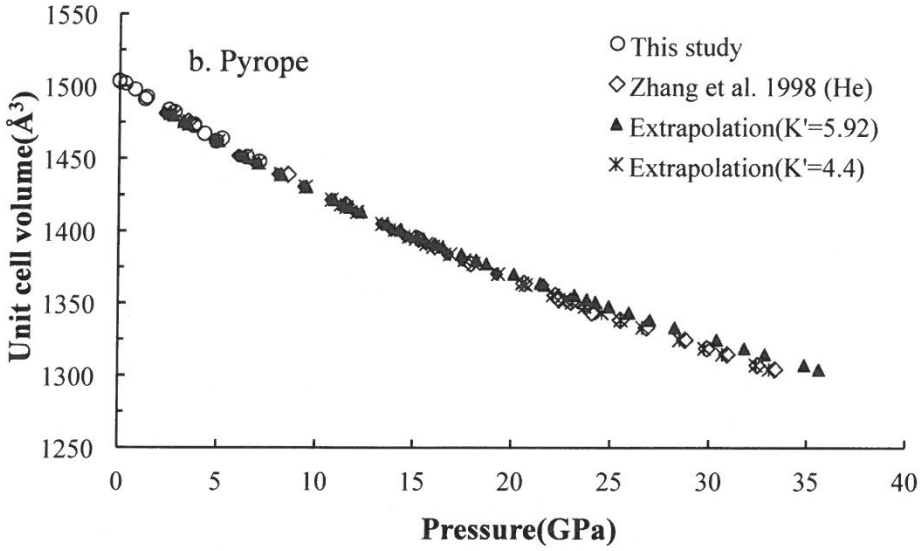
b. Pyrope
This study
Zhang et al. 1998 (He)
Extrapolation(K'=5.92)
Extrapolation(K'=4.4)
Unit cell volume(Å3)
Pressure(GPa)
1550
1500
1450
1400
1350
1300
1250
0
5
10
15
20
25
30
35
40

FIGURE 7.

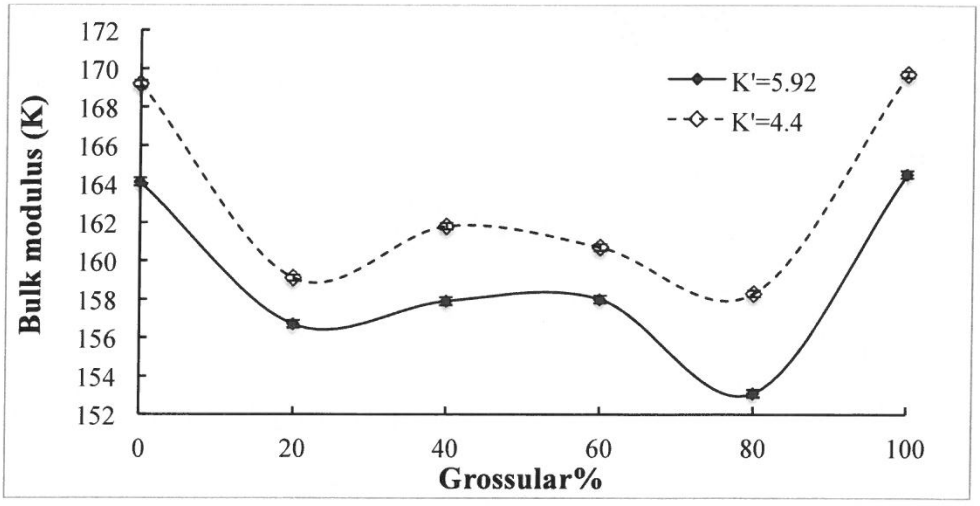
K'=5.92
K'=4.4
Bulk modulus (K)
Grossular%
172
170
168
166
164
162
160
158
156
154
152
0
20
40
60
80
100

FIGURE 8.

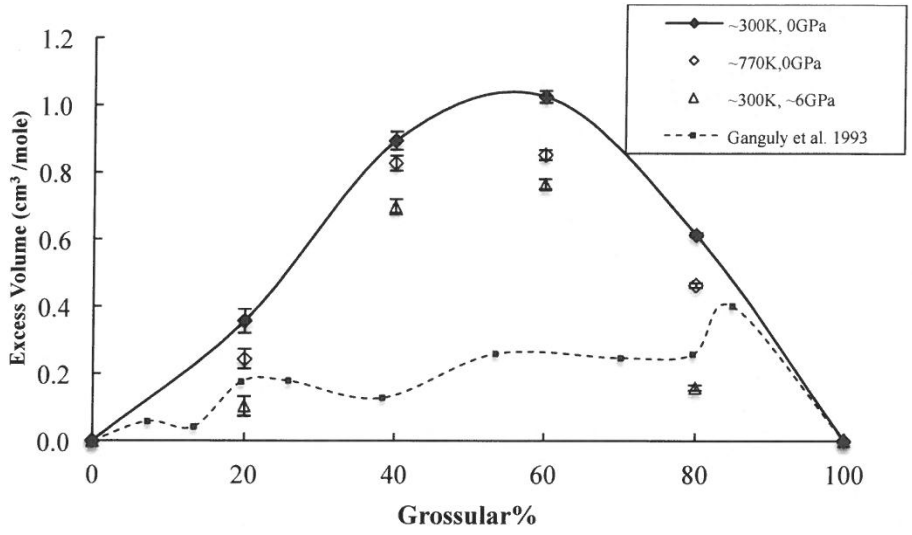
~300K, 0GPa
~770K,0GPa
~300K, ~6GPa
Ganguly et al. 1993
Excess Volume (cm³ /mole)
1.2
1.0
0.8
0.6
0.4
0.2
0.0
0
20
40
60
80
100
Grossular%